用することによりDLIの副作用であるGvHDを抑制し，担癌動物に対して延命効果を発揮することを発見している[21-23]．

## 胸腺移植併用効果

著者らは，①骨髄細胞(HSC＋MSCを含む)，②胸腺，③環境，の3つが異なったトリプルキメラマウスの系においても，移植後長期間にわたって免疫学的寛容が誘導されることを証明した[24]．この事実は将来，脳死者から高齢者(胸腺の萎縮を認める)に対してIBM-BMTをする際，流産した第三者の胎児期胸腺(両親の許可を得て使用)の移植を併用することにより，高齢者の難病治療に役立てうる重要な発見と考える．

また著者らは，IBM-BMTによってドナー由来の間葉系の細胞が胸腺へ移住し，胸腺上皮に分化することを見出した[25]．この胸腺上皮はpositive selectionのみならず，negative selectionにも関与していることが判明している．

さらに著者らは，IBM-BMTに成体胸腺移植(持続的なドナーリンパ球輸注を目的として)を併用することによって，GvHDは抑制するが，強力な抗腫瘍効果を引き出せることを発見している[26]．

また，IBM-BMTと成体胸腺移植の併用は，mildな前処置(低放射線量＋低細胞数)でもアロの骨髄細胞を生着させ，長期の生存が可能となることを見出している[27]．

最近，著者らはIBM-BMT法に胸腺移植を併用すると，加齢に伴って発症してくるAlzheimer病や，2型糖尿病の進行を抑えることを発見した[28,29]．このようにBMTと胸腺移植，さらには臓器移植を組み合わせれば将来，かなりの難治性の疾患が治療可能と考えられる．

## 最近の国内外の動向

最近，臍帯血を腸骨内へ注入する腸骨内臍帯血移植がアメリカ[30]，イタリア[31]をはじめ，わが国の数カ所の施設でも開始されるようになった．しかし，この方法には2つの欠点がある．ひとつは臍帯血中にはストローマ細胞(MSCを含む)が骨髄細胞と比較してはるかに少量であること，もうひとつは血管の豊富な腸骨内への臍帯血移植は脛骨内BMTと異なり，移植細胞が骨髄内へtrapされずに循環系へと移行しやすいという点である．以上の理由で，著者らは灌流法で採取した純粋の骨髄細胞を脛骨内へ移植する脛骨内BMT法を推奨してきた．腸骨であれ脛骨であれ，ヒトでも骨髄内への造血系細胞を直接注入する技術の安全性が，国際的にも証明されつつあるものと考えられる．

今後，脳死や心臓死の症例だけでなく，ボランティアから骨髄細胞が灌流法で採取され，移植に利用されることを期待する．

## おわりに

新移植技術(灌流法＋IBM-BMT)の特徴としては，灌流法での骨髄採取によって末梢血の混入が少ないこと，したがってGvHDが起こらないこと，一方，IBM-BMTを用いることによって効率よく，ドナーのHSCとMSCが移植可能であることがあげられる．それゆえ，造血幹細胞異常症のみならず，間葉系幹細胞異常症(加齢に伴って発症する疾患)の根治療法として，この新移植技術がクローズアップされてきている．

ヒトへの臨床応用としては現在，灌流法＋IBM-BMTの両技術のコンビネーションにおける安全性を最重点課題として，phase I studyを開始した．安全性が確認されればただちにphase II studyが実施できるように，臨床プロトコールを準備中である．新しいBMTの方法がヒトへ応用されるようになれば，骨髄ドナーの負担が軽減される．すなわち，骨髄穿刺針の穿刺部位が8カ所(従来の方法では100カ所以上)ですみ，麻酔からの覚醒後には痛みも少なく，歩行可能である[12]．それゆえ，骨髄バンクへの登録者が増加するし，たとえ，HLAが不一致でも新しい移植方法ではGvHDも起こらず，生着が促進されるため，前処置も軽減され，患者の負担も少なくなる．新技術により，これまで不治の病であった種々の難病が根治されれば，患者にとってこれ以上の福音はない．

### 文献

1) Ikehara, S. et al.: *Proc. Natl. Acad. Sci. USA*, **82**:

2483-2487, 1985.
2) Ikehara, S. et al.: *Proc. Natl. Acad. Sci. USA*, **87**: 8341-8344, 1990.
3) Than, S. et al.: *J. Exp. Med.*, **176**: 1233-1303, 1992.
4) Nishimura, A. et al.: *J. Exp. Med.*, **179**: 1053-1058, 1994.
5) Theofilopoulos, A. N. et al.: *J. Exp. Med.*, **153**: 1405-1414, 1981.
6) Ikehara, S. et al.: *Proc. Natl. Acad. Sci. USA*, **86**: 3306-3310, 1989.
7) Doi, H. et al.: *Proc. Natl. Acad. Sci. USA*, **94**: 2513-2517, 1997.
8) Hashimoto, F. et al.: *Blood*, **89**: 49-54, 1997.
9) Sugiura, K. et al.: *Stem Cells*, **19**: 46-58, 2001.
0) Kushida, T. et al.: *Blood*, **97**: 3292-3299, 2001.
1) Kushida, T. et al.: *Stem Cells*, **20**: 155-162, 2002.
2) Li, C. et al.: *Int. J. Haematol.*, **85**: 73-77, 2007.
3) Mori, S. et al.: *Int. J. Haematol.*, **93**: 822-824, 2011.
4) Nakamura, T. et al.: *Proc. Natl. Acad. Sci. USA*, **83**: 4529-4532, 1986.
5) Ildstad, S. T. et al.: *Nature*, **307**: 168-170, 1984.
16) Ikebukuro, K. et al.: *Transplantation*, **73**: 512-518, 2002.
17) Ikehara, S. et al.: *J. Autoimmun.*, **30**: 108-115, 2008.
18) Ueda, K. et al.: *Mol. Ther.*, **10**: 469-477, 2004.
19) Adachi, Y. et al.: *Stem Cells*, **24**: 2071-2077, 2006.
20) Ikehara, S. et al.: *Ann. NY Acad. Sci. USA*, **1173**: 774-780, 2009.
21) Suzuki, Y. et al.: *Stem Cells*, **23**: 365-370, 2005.
22) Koike, Y. et al.: *Stem Cells*, **25**: 385-391, 2007.
23) Mukaide, H. et al.: *Int. J. Oncol.*, **30**: 1309-1315, 2007.
24) Cui, W. et al.: *Transplantation*, **85**: 1151-1158, 2008.
25) Takaki, T. et al.: *J. Autoimmun.*, **31**: 408-415, 2008.
26) Miyake, T. et al.: *Immunology*, **126**: 552-564, 2009.
27) Nishida, T. et al.: *Bone Marrow Transplant.*, **43**: 829-837, 2009.
28) Li, M. et al.: *Neurosic. Lett.*, **465**: 36-40, 2009.
29) Li, M. et al.: *J. Autoimmun.*, **35**: 414-423, 2010.
30) Wagner, J. E. et al.: *Lancet Oncol.*, **9**: 812-814, 2008.
31) Frassoni, F. et al.: *Lancet Oncol.*, **9**: 831-839, 2008.

*　　*　　*

Best Practice & Research Clinical Haematology 24 (2011) 477–483

Contents lists available at ScienceDirect

Best Practice & Research Clinical Haematology

journal homepage: www.elsevier.com/locate/beha

17

# A novel BMT technique for treatment of various currently intractable diseases

Susumu Ikehara, Professor *

*Department of Stem Cell Disorders, Kansai Medical University, 10-15 Fumizono-cho, Moriguchi City, Osaka 570 8506, Japan*

*Keywords:*
bone marrow transplantation (BMT)
stem cell disorder (SCD)
hemopoietic stem cell (HSC)
mesenchymal stem cell (MSC)
aspiration method (AM)
perfusion method (PM)
intra-bone marrow (IBM)
autoimmune disease
osteoporosis
emphysema

A recently-developed BMT method combines a "Perfusion Method" (PM) for collecting bone marrow cells (BMCs) with the Intra-Bone Marrow (IBM) injection of BMCs (IBM-BMT). As distinct from the conventional aspiration method (AM), the PM allows rapid (within 1 h) collection of BMCs without T cell contamination (T cells < 10%). Therefore, no GvHD occurs. Moreover, the burden on donors, such as back pain, bleeding and infection, can be reduced.

Full chimerism can be achieved even with only mild conditioning regimens if IBM-BMT is carried out, since IBM-BMT replaces not only the recipient's hemopoietic stem cells (HSCs) but also mesenchymal stem cells (MSCs) with donor-derived HSCs and MSCs.

Using this method, we show that most currently intractable diseases are HSC or MSC disorders, and that this novel strategy (PM + IBM–BMT) can be used to treat various otherwise intractable diseases (including autoimmune diseases and age-associated diseases).

We believe that the development of this technique will herald a revolution in the field of BMT, regeneration medicine and also organ transplantation.



## Introduction

In 1985, we found that allogeneic bone marrow transplantation (BMT) (but not autologous BMT) could be used to prevent and treat autoimmune diseases in autoimmune-prone mice [1,2]. In addition, we succeeded in inducing autoimmune diseases in normal mice by the transplantation of T cell-

* Tel.: +81 6 6993 9625; Fax: +81 6 6993 9627.
*E-mail address:* ikehara@takii.kmu.ac.jp.

1521-6926/$ – see front matter © 2011 Elsevier Ltd. All rights reserved.
doi:10.1016/j.beha.2011.04.003

depleted bone marrow cells (BMCs) or partially purified hemopoietic stem cells (HSCs) from autoimmune-prone mice to normal mice [3,4].

Based on these findings, we have proposed that autoimmune diseases originate from defects in HSCs [3–7], and have also found that abnormal HSCs of autoimmune-prone mice are more resilient than normal HSCs [4,8,9]; abnormal HSCs can proliferate even in the allogeneic microenvironments, whilst normal HSCs can proliferate in collaboration with major histocompatibility complex (MHC)-compatible stromal cells (mesenchymal stem cells: MSCs), but not MHC-incompatible MSCs [4,8,9].

From these findings, we realized that, in the case of BMT across MHC barriers, we would have to transplant both donor-derived HSCs and MSCs to ensure that the donor-derived normal HSCs grow and survive in the allogeneic environments.

Recently, we have discovered that the injection of whole BMCs directly into the bone cavity (intra-bone marrow-BMT: IBM-BMT) provides distinct advantages, since IBM-BMT can efficiently recruit not only donor-derived HSCs but also MSCs. We here review our data regarding IBM-BMT plus the perfusion method (PM) (capable of efficiently collecting MSCs).

*Advantages of novel BMT*

As shown in Fig. 1, conventional BMT is carried out as follows: Bone marrow needles are inserted into the iliac bones more than 100 times, and the BMCs are collected by the aspiration method (AM). Therefore, contamination with peripheral blood (particularly T cells) is inevitable. When thus-collected cells are intravenously injected (IV-BMT), most cells become trapped in the lung and only a few cells migrate into the bone marrow (Fig. 1).

To apply our new BMT methods to humans, we established, using cynomolgus monkeys, a "PM", which minimizes the contamination of BMCs with T cells. As shown in Fig. 2, two needles are inserted into a long bone such as the humerus, femur, or tibia. The end of the extension tube is connected to a needle. The other end is placed in a syringe containing 0.5 ml heparin. The other needle is connected to a syringe containing 30 ml of saline, and the saline is then pushed gently from the syringe into the medullary cavity to flush out the bone marrow (BM). The saline containing the BM fluid is then collected.

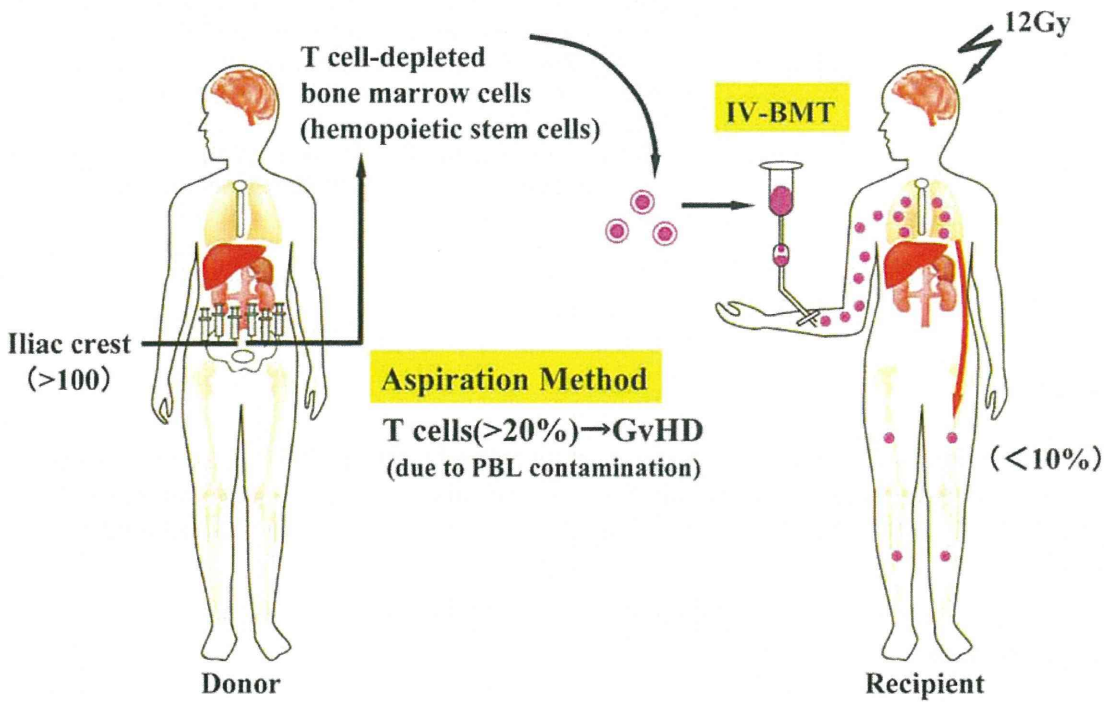


**Fig. 1.** Conventional BMT for allogeneic BMT. Conventional BMT is carried out using an aspiration method (AM), followed by the intravenous injection of BMCs (IV-BMT).

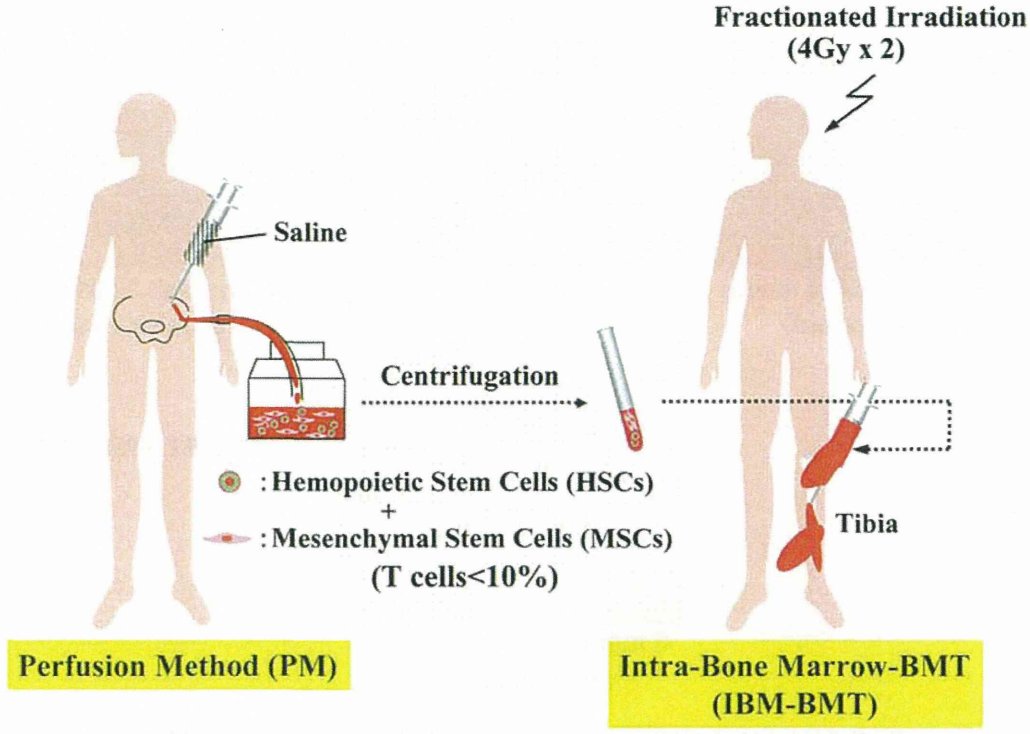


**Fig. 2.** New BMT method for allogeneic BMT. The new BMT method is carried out using a perfusion method (PM), followed by IBM–BMT.

There is significantly less contamination with T cells when using the PM (<10%) than with the conventional AM (>20%) [10,11]. Therefore, T cell-depletion is unnecessary with the PM, and whole BMCs can be used. However, in the case of the conventional AM, T cell-depletion is necessary, and the loss of some important cells such as MSCs during the process of T cell-depletion is inevitable. Furthermore, the number and progenitor activities of the cells harvested using the PM are greater than when using the conventional AM [10,11].

We have also found that the PM is applicable to the iliac bones as well as the long bones not only in monkeys but also in humans.

We are now starting a Phase I Study for the clinical application of PM + IBM–BMT.

*IBM–BMT for organ transplantation*

Since we have previously found that the combination of organ allografts and conventional IV-BMT from the same donors prevents the rejection of organ allografts [12], we attempted to apply IBM–BMT to organ allografts. IBM–BMT was the most effective strategy, since the radiation dose could be reduced to 4.0Gy × 2 in skin allografts [12,13]. In addition, we found that IBM–BMT is applicable to allografts of other organs and tissues in rats, such as pancreas islets [14] legs [15], lungs [16], and heart [17].

*IBM–BMT for regeneration therapy*

As it was apparent that donor stromal cells could be effectively recruited by "IBM–BMT", we next attempted to treat osteoporosis in SAMP6 mice; the SAMP6 mouse (a substrain of senescence-accelerated mice) spontaneously develops osteoporosis early in life and is therefore a useful model for examining the mechanisms underlying osteoporosis. After IBM–BMT, the hematolymphoid system was completely reconstituted with donor-type cells. Thus-treated SAMP6 mice (8 months after IBM-BMT) showed marked increases in trabecular bone even at 20 months of age (Fig. 3), and the bone mineral density (BMD) remained similar to that of normal B6 mice. Bone marrow stromal cells in "IBM-

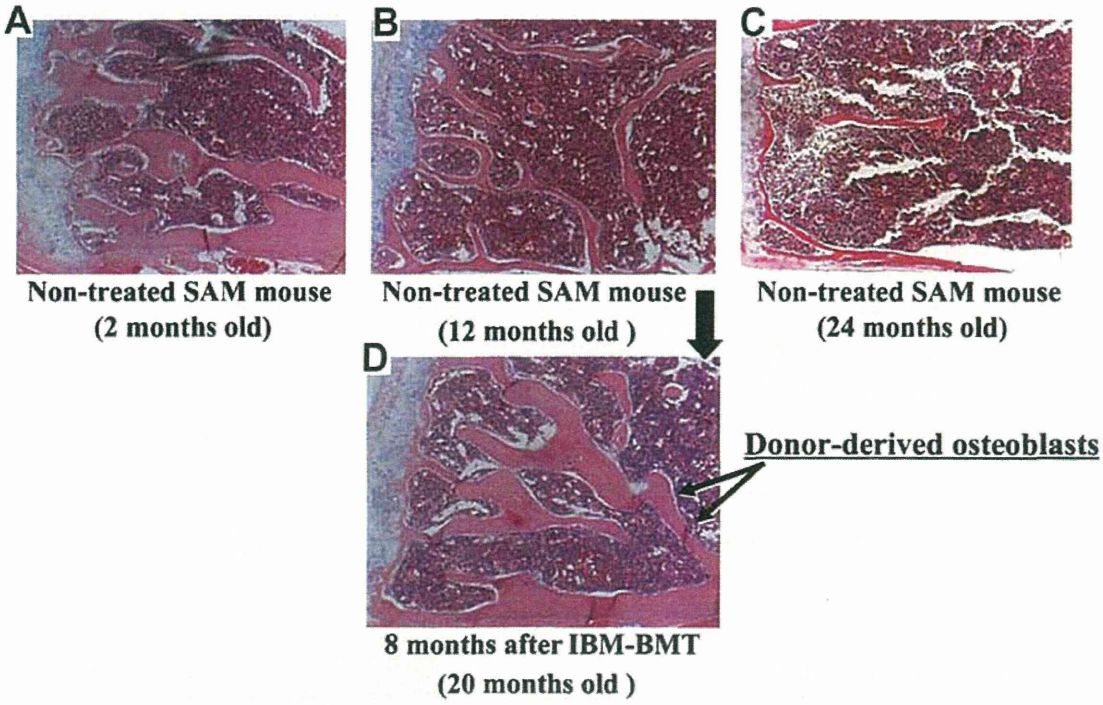


**Fig. 3.** Treatment of osteoporosis in SAMP6 mice by IBM–BMT from normal B6 mice.

BMT"-treated SAMP6 mice were replaced by donor stromal cells [18,19]. Thus, we succeeded in curing osteoporosis in SAMP6 mice by IBM–BMT, which can recruit both donor-derived HSCs and MSCs.

Since IBM–BMT appeared to be a powerful strategy in regeneration therapy, we next used tight-skin (Tsk) mice (an animal model for emphysema) to examine whether emphysema could be cured by IBM–BMT.

IBM-BMT was carried out from C3H mice into Tsk mice (8–10 weeks old) that had already shown emphysema. Eight months after the transplantation, the lungs of all the Tsk mice treated with IBM-BMT [C3H→Tsk] showed structures similar to those of normal mice, whereas the [Tsk→Tsk] mice showed emphysema, as seen in age-matched Tsk mice. Next, we attempted to transfer emphysema from Tsk mice to C3H mice by IBM–BMT. Six months after IBM-BMT, the [Tsk→C3H] mice showed emphysema [20]. These results strongly suggested that emphysema in Tsk mice originates from defects in the stem cells (probably MSCs and/or HSCs) in the bone marrow [20].

### *IBM–BMT + donor lymphocyte infusion (DLI) for treatment of malignant tumors*

It is well known that the graft-versus-leukemia reaction (GvLR) can cure patients of a variety of hematological malignancies [21,22]. Recently, it has been reported that graft-versus-tumor (GvT) effects can induce partial (complete in some) remission of metastatic solid tumors such as breast cancer [23–25] and renal cell carcinoma [26–30]. Based on these findings, donor lymphocyte infusion (DLI) has recently been used for the treatment of malignant solid tumors even in humans. However, it is very difficult to completely eradicate the tumors, since extensive DLI induces graft-versus-host disease (GvHD). We therefore attempted to establish a new method for the treatment of malignant tumors, this method consisting of intra-bone marrow-IBM–BMT plus DLI, since we have recently found that IBM-BMT can allow a reduction in radiation doses as a conditioning regimen and prevent GvHD [31,32]. Using the Meth-A cell line (BALB/c-derived fibrosarcoma), we found that IBM-BMT plus the injection of $CD4^+$ T-cell-depleted (but not $CD8^+$ T-cell-depleted) spleen cells (as DLI) can prevent GvHD while suppressing tumor growth [33] (Fig. 4). In addition, we have found that IBM-BMT plus extensive DLI (3

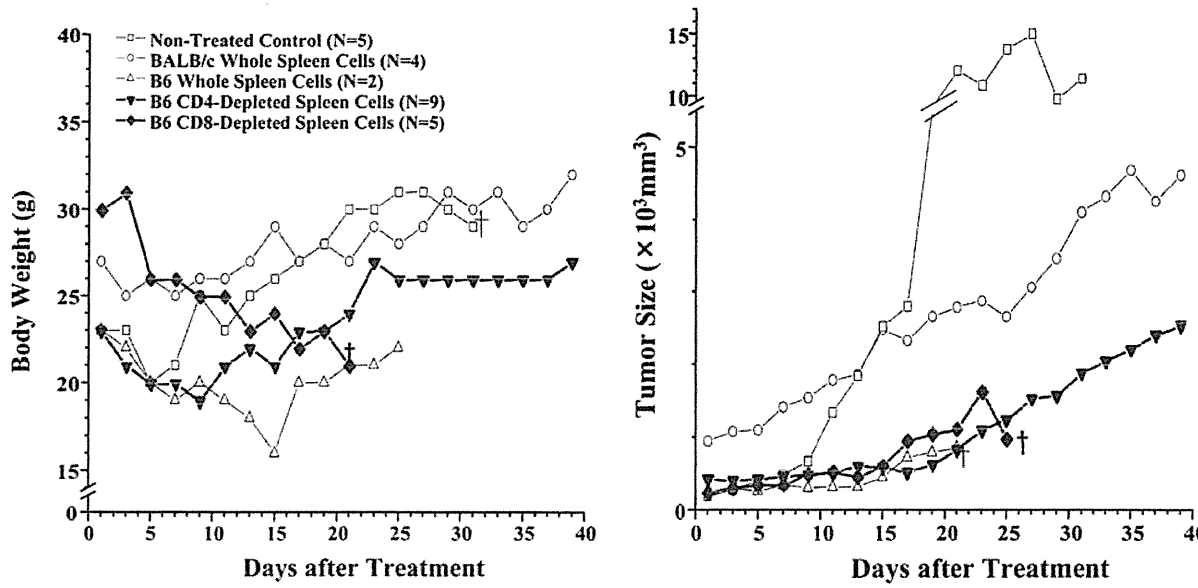


**Fig. 4.** Prevention of GvHD and suppression of tumor growth by IBM–BMT + DLI ($CD4^-$).

times every 2 weeks) leads to the complete rejection of the tumor, although the success rate (3/50) is not high so far [33].

In addition, we have examined whether this strategy (IBM-BMT plus DLI) is applicable to other tumors in other animals. We have obtained similar results in another system (colon cancer: ACL-15 in rats) [34]. We are now establishing more efficient strategies to eradicate malignant tumors.

*IBM–BMT + thymus transplantation (TT) for modulation of age-associated diseases*

We have recently proposed that age-associated diseases (AADs), such as osteoporosis and emphysema, are mesenchymal stem cell disorders.

Based on our findings, we attempted to prevent the progression of Alzheimer's disease using senescence-accelerated mice by IBM-BMT, and succeeded in preventing the development of Alzheimer's disease [35].

In addition, we succeeded in curing type 2 diabetes mellitus in db/db mice by IBM-BMT with TT [36].

These findings suggest that TT plays a crucial role in the prevention and treatment of AADs, since the recovery of T cell functions would be delayed after IBM–BMT alone (but not after IBM–BMT + TT).

## Future directions

As described here, the new BMT method (PM + IBM–BMT) can be used to treat various otherwise intractable diseases, including i) autoimmune diseases, ii) AADs (osteoporosis, emphysema, etc.), iii) diseases curable by organ transplantation and iv) malignant tumors (including solid tumors) [33]. The PM can efficiently be used to collect whole BMCs (including HSCs and MSCs) without them being contaminated with T cells, and no GVHD therefore develops. IBM-BMT can efficiently transfer donor whole BMCs (both HSCs and MSCs) into recipients, and this method can therefore be used to quickly replace not only HSCs but also MSCs with donor-derived cells.

From the findings to date, it is conceivable that all the body's cells originate in the bone marrow, and that all diseases might therefore originate from defects in the bone marrow. One paper already suggests that gastric cancer originates from bone marrow-derived cells [37].

We believe that the development of our BMT method heralds a revolution in the field of transplantation (BMT and organ transplantation) and regeneration therapy.

## Conflict of interest

No conflicts of interest to declare.

## Acknowledgments

I thank Mr. Hilary Eastwick-Field and Ms. K. Ando for their help in the preparation of the manuscript. These studies were mainly supported by the 21st Century Center of Excellence (COE) program of the Ministry of Education, Culture, Sports, Science and Technology. Supported also by a grant from Haiteku Research Center of the Ministry of Education, Health and Labour Sciences Research Grants, a grant from the Science Frontier program of the Ministry of Education, Culture, Sports, Science and Technology, and a grant from the Department of Transplantation for Regeneration Therapy (sponsored by Otsuka Pharmaceutical Company, Ltd.), a grant from Molecular Medical Science Institute, Otsuka Pharmaceutical Co., Ltd., and a grant from Japan Immunoresearch Laboratories Co., Ltd. (JIMRO).

## References

*[1] Ikehara S, Good RA, Nakamura T, et al. Rationale for bone marrow transplantation in the treatment of autoimmune diseases. Proc Natl Acad Sci USA 1985 Apr;82(8):2483–7.
[2] Ikehara S, Ohtsuki H, Good RA, et al. Prevention of type I diabetes in nonobese diabetic mice by allogeneic bone marrow transplantation. Proc Natl Acad Sci USA 1985 Nov;82(22):7743–7.
*[3] Ikehara S, Kawamura M, Takao F, et al. Organ-specific and systemic autoimmune diseases originate from defects in hematopoietic stem cells. Proc Natl Acad Sci USA 1990 Nov;87(21):8341–4.
[4] Kawamura M, Hisha H, Li Y, et al. Distinct qualitative differences between normal and abnormal hemopoietic stem cells in vivo and in vitro. Stem Cells 1997 Jan;15(1):56–62.
[5] Ikehara S. Autoimmune diseases as "stem cell disorders". Acta Histochem Cytochem 1997;30(1):3–12.
[6] Ikehara S. Autoimmune diseases as stem cell disorders: normal stem cell transplant for their treatment. Int J Mol Med 1998 Jan;1(1):5–16.
[7] Ikehara S. State-of-the-art review. A new concept of stem cell disorders and their new therapy. J Hematother Stem Cell Res 2003 Dec;12(6):643–53.
*[8] Hashimoto F, Sugiura K, Inoue K, et al. Major histocompatibility complex restriction between hematopoietic stem cells and stromal cells in vivo. Blood 1997 Jan;89(1):49–54.
[9] Sugiura K, Hisha H, Ishikawa J, et al. Major histocompatibility complex restriction between hematopoietic stem cells and stromal cells in vitro. Stem Cells 2001 Jan;19(1):46–58.
*[10] Inaba M, Adachi Y, Hisha H, et al. Extensive studies on perfusion metgod plus itra-bone marrow-bone marrow transplantation using cynomolgus monkeys. Stem Cells 2007 Aug;25(8):2098–103.
[11] Kushida T, Inaba M, Ikebukuro K, et al. Comparison of bone marrow cells harvested from various bones of cynomolgus monkeys of various ages by perfusion or aspiration methods: a preclinical study for human BMT. Stem Cells 2002 Mar; 20(2):155–62.
[12] Nakamura T, Good RA, Inoue S, et al. Successful liver allografts in mice by combination with allogeneic bone marrow transplantation. Proc Natl Acad Sci USA 1986 Jan;83(12):4529–32.
*[13] Ikehara S. A novel method of bone marrow transplantation (BMT) for intractable autoimmune diseases. J Autoimmun 2008 May;30(3):108–15.
[14] Ikebukuro K, Adachi Y, Suzuki Y, et al. Synergistic effects of induction in transplantation of allogeneic pancreatic islets. Bone Marrow Transplant 2006 Nov;38(10):657–64.
[15] Esumi T, Inaba M, Ichioka N, et al. Successful allogeneic leg transplantation in rats by combination of intra-bone marrow (IBM) injection of donor bone marrow cells. Transplantation 2003 Dec;76(11):1543–8.
[16] Kaneda H, Adachi Y, Saito Y, et al. Long-term observation after simultaneous lung and intra-bone marrow-bone marrow transplantation. J Heart Lung Transplant 2005 Sept;24(9):1415–23.
[17] Guo K, Inaba M, Li M, et al. Long-term donor-specific tolerance in rat cardiac allografts by intra-bone marrow injection of donor bone marrow cells. Transplantation 2008 Jan;85(5):93–101.
[18] Ichioka N, Inaba M, Kushida T, et al. Prevention of senile osteoporosis in SAMP6 mice by intra-bone marrow injection of allogeneic bone marrow cells. Stem Cells 2002 Nov;20(6):542–51.
*[19] Takada K, Inaba M, Ichioka N, et al. Treatment of senile osteoporosis in SAMP6 mice by intra-bone marrow injection of allogeneic bone marrow cells. Stem Cells 2006 Feb;24(2):399–405.
*[20] Adachi Y, Oyaizu H, Taketani S, et al. Treatment and transfer of emphysema by a new bone marrow transplantation method from normal mice to Tsk mice and vice versa. Stem Cells 2006 Sep;24(9):2071–7.
[21] Thomas ED, Blume KG. Historical markers in the development of allogeneic hematopoietic cell transplantation. Biol Blood Marrow Transplant 1999 Dec;5(6):341–6.
[22] Weiden PL, Flournoy N, Thomas ED, et al. Antileukemic effect of graft-versus-host diseases in human recipients of allogeneic-marrow grafts. N Engl J Med 1979 May;300(19):1068–73.
[23] Ben-Yosef R, Or R, Nagker A, et al. Graft-versus-tumor and graft-versus-leukaemia effect in patient with concurrent breast cancer and acute myelocytic leukaemia. Lancet 1996 Nov. 29;348(9036):1242–3.
[24] Eibi B, Schwaigofer H, Nachbaur D, et al. Evidence for a graft-versus-tumor effect in a patient treated with marrow ablative chemotherapy and allogeneic bone marrow transplantation for breast cancer. Blood 1996 Aug;88(4):1501–8.

[25] Ueno NT, Rondon G, Mirza NQ, et al. Allogeneic peripheral-blood progenitor-cell transplantation for poor-risk patients with metastatic breast cancer. J Clin Oncol 1998 Mar;16(3):986–93.
[26] Childs RW, Clave E, Tisdale J, et al. Successful treatment of metastatic renal cell carcinoma with a nonmyeloablative allogeneic peripheral-blood progenitor-cell transplant: evidence for a graft-versus-tumor effect. J Clin Oncol 1999 Jul; 17(7):2044–9.
[27] Childs R, Chernoff A, Contentin N, et al. Regression of metastatic renal-cell carcinoma after nonmyeloablative allogeneic peripheral-blood stem-cell transplantation. N Engl J Med 2000 Sept. 14;343(11):750–8.
[28] Appelbaum FR, Sandmaier B. Sensitivity of renal cell cancer to nonmyeloablative allogeneic hematopoietic cell transplantation: unusual or unusually important? J Clin Oncol 2002 Apr. 15;20(8):1965–7.
[29] Bregni M, Dodero A, Peccatori J, et al. Nonmyeloablative conditioning followed by hematopoietic cell allografting and donor lymphocyte infusions for patients with metastatic renal and breast cancer. Blood 2002 Jun. 1;99(11):4234–6.
[30] Hentschke P, Barkholt L, Uzunel M, et al. Low-intensity conditioning and hematopoietic stem cell transplantation in patients with renal and colon carcinoma. Bone Marrow Transplant 2003 Feb;31(4):253–61.
*[31] Kushida T, Inaba M, Hisha H, et al. Intra-bone marrow injection of allogeneic bone marrow cells: a powerful new strategy for treatment of intractable autoimmune diseases in MRL/lpr mice. Blood 2001 May;97(10):3292–9.
[32] Rini BI, Zimmerman T, Stadler WM, et al. Allogeneic stem-cell transplantation of renal cell cancer after nonmyeloablative chemotherapy: feasibility, engraftment, and clinical results. J Clin Oncol 2002 Apr. 15;20(8):2017–24.
*[33] Suzuki Y, Adachi Y, Minamino K, et al. A new strategy for treatment of malignant tumor: intra-bone marrow-bone marrow transplantation plus $CD4^-$ donor lymphocyte infusion. Stem Cells 2005 Mar;23(3):365–70.
[34] Koike Y, Adachi Y, Suzuki Y, et al. Allogeneic intra-bone marrow-bone marrow transplantation plus donor lymphocyte infusion suppresses growth of colon cancer cells implanted in skin and liver of rats. Stem Cells 2007 Feb;25(2):385–91.
[35] Li M, Inaba M, Guo K, et al. Amelioration of cognitive ability in senescence-accelerated mouse prone 8 (SAMP8) by intra-bone marrow-bone marrow transplantation. Neurosci Lett 2009 Nov. 6;465(1):36–40.
*[36] Li M, Abraham NG, Vanella L, et al. Successful modulation of type 2 diabetes in db/db mice with intra-bone marrow-bone marrow transplantation plus concurrent thymic transplantation. J Autoimmun; 2010 Sep 28 [Epub ahead of print].
[37] Houghton J, Stoicov C, Nomura S, et al. Gastric cancer originating from bone marrow-derived cells. Science 2004 nov. 26; 306(5701):1568–71.

J Gastroenterol (2011) 46:1368–1381
DOI 10.1007/s00535-011-0460-4

ORIGINAL ARTICLE—ALIMENTARY TRACT

# Amelioration of 2,4,6-trinitrobenzene sulfonic acid-induced colitis in mice by immunoregulatory dendritic cells

**Shoichi Hoshino · Akiko Kurishima · Muneo Inaba · Yugo Ando · Toshiro Fukui · Kazushige Uchida · Akiyoshi Nishio · Hiroshi Iwai · Takashi Yokoi · Tomoki Ito · Sanae Hasegawa-Ishii · Atsuyoshi Shimada · Ming Li · Kazuichi Okazaki · Susumu Ikehara**

Received: 13 July 2010 / Accepted: 17 July 2011 / Published online: 16 September 2011


**Abstract**
*Background* Dendritic cells (DCs) are widely distributed throughout the lymphoid and nonlymphoid tissues, and are important initiators of acquired immunity. They also serve as regulators by inducing self-tolerance. However, it has not been thoroughly clarified whether DCs are somehow involved in the regulation or treatment of inflammatory bowel diseases.

*Methods* We established an ileitis model by transmurally injecting 2,4,6-trinitrobenzene sulfonic acid (TNBS) into the lumen of the ileocolonic junction. The kinetic movement of DCs at the inflammatory sites was analyzed histologically and by flow cytometry, and DCs obtained from the small intestine were analyzed in order to determine the expression of paired immunoglobulin-like receptor-A/B (PIR-A/B) by flow cytometry and quantitative RT-PCR. Furthermore, the regulatory role of DCs was directly determined by a transfer experiment using TNBS-induced colitis model mice.

S. Hoshino and A. Kurishima contributed equally to this work.

S. Hoshino · A. Kurishima · Y. Ando · T. Fukui · K. Uchida · A. Nishio · K. Okazaki
The Third Department of Internal Medicine, Division of Gastroenterology and Hepatology, Kansai Medical University, Moriguchi, Osaka, Japan
e-mail: hoshinos@takii.kmu.ac.jp

A. Kurishima
e-mail: kurishia@takii.kmu.ac.jp

T. Fukui
e-mail: fukuitos@takii.kmu.ac.jp

K. Uchida
e-mail: uchidak@takii.kmu.ac.jp

A. Nishio
e-mail: nishioa@takii.kmu.ac.jp

K. Okazaki
e-mail: okazaki@hirakata.kmu.ac.jp

M. Inaba
First Department of Pathology, Kansai Medical University, Moriguchi, Osaka, Japan
e-mail: inabam@takii.kmu.ac.jp

H. Iwai
Department of Otolaryngology, Kansai Medical University, Moriguchi, Osaka, Japan
e-mail: iwai@takii.kmu.ac.jp

T. Yokoi · T. Ito
First Department of Internal Medicine, Kansai Medical University, Moriguchi, Osaka, Japan
e-mail: yokoit@hirakata.kmu.ac.jp

T. Ito
e-mail: itot@takii.kmu.ac.jp

S. Hasegawa-Ishii · A. Shimada
Department of Pathology, Institute for Developmental Research, Aichi Human Service Center, Kasugai, Aichi, Japan
e-mail: sanae@inst-hsc.jp

A. Shimada
e-mail: ats7@ma.ccnw.ne.jp

M. Li · S. Ikehara (✉)
Department of Stem Cell Disorders, Kansai Medical University, 10-15 Fumizono-cho, Moriguchi, Osaka 570-8506, Japan
e-mail: ikehara@takii.kmu.ac.jp

M. Li
e-mail: liming@takii.kmu.ac.jp

*Results* We observed three DC subsets (PIR-A/B$^{high}$, PIR-A/B$^{med}$, and PIR-A/B$^{-}$ DCs) in the conventional DCs (cDCs) from day 3, and the number of PIR-A/B$^{med}$ cDCs increased from the time the inflammatory responses ceased (day 7). PIR-A/B$^{med}$ cDCs actually migrated to the inflamed colon, and ameliorated the colitis induced by TNBS when transferred to colitis-induced recipients. The colitis was greatly exacerbated when mice had been treated with the indoleamine-pyrrole 2,3-dioxygenase (IDO) inhibitor 1-methyltryptophan (1-mT) at the time PIR-A/B$^{med}$ cDCs were transferred, indicating that the therapeutic ability of PIR-A/B$^{med}$ cDCs is partially dependent on IDO.
*Conclusion* The PIR-A/B$^{med}$ cDCs, which increase in number during the final stages of inflammation, can be used to treat colitis via an IDO-dependent mechanism.

**Keywords** Dendritic cells · Paired immunoglobulin-like receptors · TNBS · Inflammatory bowel disease

## Introduction

The function of mucosal dendritic cells (DCs) is tightly regulated by the local microenvironment, which includes immune cells, nonimmune cells, and luminal bacteria. Since mucosal DCs are more effective at presenting antigens than epithelial cells, they are likely to be key players in gut immune homeostasis.

Previously, we examined the kinetic movement of DCs in the lamina propria from the viewpoint of their expression of dual-functioning paired immunoglobulin-like receptors (PIR) in the 2,4,6-trinitrobenzene sulfonic acid (TNBS)-induced ileitis model (an animal model of Crohn's disease) [1]. We observed three subsets of DCs (PIR-A/B$^{high}$, PIR-A/B$^{med}$, and PIR-A/B$^{-}$) in the CD11c$^{+}$/B220$^{-}$ conventional DCs (cDCs). The PIR-A/B$^{med}$ cDCs, which increase in number during the final stages of inflammation, might be involved in the termination of the TNBS-induced ileitis by the delivery of anergic signals to effector T cells as a result of the lower expressions of costimulatory molecules and the production of immunoregulatory cytokine.

In our previous paper, we examined the role of the immunoregulatory PIR-A/B$^{med}$ DC subset on the expression of some surface markers [1]. Recently, a new classification of DCs has been emerging—one based mainly on the origin of the DC subsets. One subset of DCs consists of cells with CD103$^{+}$CX$_3$CR1$^{-}$, which arise from DC-committed precursors (pre-DCs) and common monocyte and dendritic cell precursors under the influence of Flt3 ligand. A second DC subset consists of cells that are CD11b$^{+}$CD14$^{+}$CX$_3$CR1$^{+}$ and that are derived from Ly6$^{lo}$ monocytes driven by GM-CSF [2–4].

Of note is that CD103$^{+}$ DCs migrate into the draining mesenteric lymph nodes where they promote the conversion of Foxp3$^{+}$ regulatory T (Treg) cells in a retinoic acid (RA)- and TGF-$\beta$-dependent manner [5–7]. Thus, to further characterize our unique DC subset—immunoregulatory PIR-A/B$^{med}$ DCs in the small intestine—from various aspects, we analyzed the expression of these DC stage-specific surface molecules (CD103, CX$_3$CR1, and CD11b) on this DC subset and compared their levels with the other DC subsets, this being important in order to evaluate the immunoregulatory functions of PIR-A/B$^{med}$ DCs.

Also of importance is to investigate whether this newly discovered DC subset in the small intestine actually ameliorates (or prevents) the intestinal inflammation. In this paper we describe the adoptive cell transfer of PIR-A/B$^{med}$ cDCs into mice with TNBS-induced colitis and the various indices including mortality, changes in body weight, macroscopical appearances, and histological changes, which were markedly improved in the recipients of PIR-A/B$^{med}$ cDCs, but not in the recipients of the other DC subsets, suggesting the therapeutic role of PIR-A/B$^{med}$ cDCs. This result paves the way for future research focusing on this DC subset.

## Materials and methods

### Surface marker analyses

Small intestine (SI)-derived DC-enriched cells were isolated as previously described [1, 8]. The cells were stained with fluorescein isothiocyanate (FITC)-conjugated mAb against CD11c (BD Biosciences, San Jose, CA), phycoerythrin (PE)-conjugated anti-CD11c, -CD103, PIR-A/B (BD Biosciences), PIR-B (clone 326414: R&D Systems, Inc., Minneapolis, USA), and allophycocyanin (APC)-conjugated anti-CD45R (B220) (BD Biosciences), -CD11b, -CD83 mAbs (eBioscience Inc., San Diego, CA), -CD40, -CD86, and -CD197 mAbs (CCR7), Alexa Fluor 647-conjugated anti-CD54 mAbs, PE/Cy7-conjugated anti-CD86 mAbs (BioLegend, San Diego, CA, USA), -CD45R (B220) (BD Biosciences), PIR-A/B (BD Biosciences), and anti-CX3CR1 Abs (ProSci inc., Flint Place Poway, CA, USA). The controls included the isotype-matched irrelevant mAbs labeled with the corresponding fluorochromes. The cells were analyzed using a FACS Calibur HG (Becton–Dickinson and Company, Mountain View, CA, USA). Dead cells were excluded from analysis using propidium iodide staining.

### Isolation of SI-derived dendritic cells

SI-derived DCs were stained with FITC-anti-CD11c, PE-anti-PIR-A/B, and APC-anti-CD45R mAbs, and the cells with the PIR$^{high}$, PIR$^{med}$, and PIR$^{low/-}$ immunophenotypes in the CD11c$^{+}$ DCs were separately sorted by a FACSAria

(Becton–Dickinson and Company). In some experiments, $CD103^{low}$PIR-A/$B^{med}$ cDCs and $CD103^{high}$PIR-A/$B^{med}$ cDCs were also sorted by a FACSAria.

### Mixed leukocyte reaction

Mixed leukocyte reaction (MLR) was performed to examine the stimulatory activities of SI-derived DC subsets. MLR was performed as follows: $CD4^+$ T cells were prepared from allogeneic C57BL/6 spleen cells by using a $CD4^+$T cell isolation kit (Miltenyi Biotec GmbH). The responder splenic $CD4^+$ T cells ($2 \times 10^4$) were cultured with graded doses of irradiated (12 Gy) stimulator DCs (SI-derived DCs or splenic DCs) for 72 h and pulsed with 0.5 μCi of [$^3$H]thymidine for the last 16 h of the culturing period. Splenic DCs, isolated as $CD11c^+/CD3^-/B220^-$ cells, were used as positive control APCs.

### Induction of ileitis

Ileitis was induced by the injection of TNBS (Wako Pure Chemical Industries, Ltd., Osaka, Japan) as described previously [1, 9]. Briefly, the mice underwent a laparotomy under anesthesia. The terminal ileal loop was gently exteriorized on sterile gauze, and 70 μl of 32 mg/ml TNBS solution dissolved in 50% ethanol was then injected transmurally into the lumen 1 cm proximal to the ileocolonic junction. The laparotomy was closed in two layers using nonresorbable nylon sutures.

### Induction of colitis

BALB/c mice were purchased from Japan SLC, Inc. (Hamamatsu, Japan) and maintained in our animal facility under specific pathogen-free conditions. Colitis was induced as described previously [10]. Briefly, the mice were lightly anesthetized with pentobarbital sodium (Kyoritsu Seiyaku Corporation, Tokyo, Japan), and a 3.0-F catheter was then carefully inserted into the colon such that the tip was 4 cm proximal to the anus. To induce colitis, 80 μl of 32 mg/ml TNBS solution dissolved in 50% ethanol was slowly administered into the lumen of the colon via the catheter fitted onto a 1-ml syringe. In control experiments, mice received 50% ethanol alone using the same technique described above. Animals were then kept in a vertical position for 30 s and returned to their cages.

### Adoptive cell transfer of cDCs

SI-derived cDC subsets prepared from the ileitis-induced mice after the injection of TNBS were intraperitoneally injected into the recipients. Then $2 \times 10^5$ PIR-A/$B^{med}$ cDCs, PIR-A/$B^-$ cDCs, or $1 \times 10^4$ PIR-A/$B^{high}$ cDCs was transferred into the recipients on the basis of the proportion of three subsets prepared from the small intestine. Since the number of PIR-A/$B^{high}$ cDCs is fewer than the others in vivo, fewer PIR-A/$B^{high}$ cDCs were transferred.

In some experiments, SI-derived $PIR^{med}$ cDC subsets prepared from the ileitis-induced mice were labeled with CFSE (Vybrant CFDA SE Cell Tracer Kit, Invitrogen, Carlsbad, CA, USA) to perform the cell-tracing analysis. The labeled cells were intraperitoneally transferred into the recipients at the time when colitis was induced by TNBS. On day 3 after the transfer, we prepared the frozen sections of intestinal tissue and analyzed them using a fluorescence microscope (BX 50 research microscope, Olympus, Japan). DAPI (Nacalai Tesque Inc., Kyoto, Japan) was used to stain cellular nuclei.

### Inhibition of indoleamine-pyrrole 2,3-dioxygenase

To inhibit the activity of indoleamine-pyrrole 2,3-dioxygenase (IDO), the mice were intraperitoneally injected daily with 10 mg of 1-methyltryptophan (1-mT, dissolved in phosphate-buffered saline, Sigma Aldrich Co., St Louis, MO, USA) from day 3 (at the time when SI-derived PIR-A/$B^{med}$ cDCs were transferred) to the end of the experiment. The mice were sacrificed on day 7 to assess the morphologic and histological changes in the colon.

Furthermore, SI-derived PIR-A/$B^{med}$ cDCs were treated with 2 mM 1-mT for 24 h, and $2 \times 10^5$ PIR-A/$B^{med}$ cDCs thus treated were transferred to the ileitis-induced mice to examine the in vitro effect of 1-mT.

### Macroscopic assessment of severity of colitis

The mice were killed by cervical dislocation, the colon excised, opened longitudinally, and washed in saline. Macroscopic damage was assessed by the scoring system of Wallace and Keenan [11], which takes into account the area of inflammation and the presence or absence of ulcers. The criteria for assessing macroscopic damage was based on a semiquantitative scoring system, where features were graded as follows: 0, no ulcer, no inflammation; 1, no ulcer, local hyperemia; 2, ulceration without hyperemia; 3, ulceration and inflammation at one site only; 4, two or more sites of ulceration and inflammation; and 5, ulceration extending more than 2 cm.

### Microscopic assessment of colitis

Tissues were removed at the indicated time points and embedded in paraffin. Paraffin sections were made and stained with hematoxylin and eosin. The degree of inflammation on microscopic cross sections of the colon was graded semiquantitatively from 0 to 4 according to

previously described criteria [10] as follows: 0, no signs of inflammation; 1, very low level; and 2, low level of leukocytic infiltration; 3, high level of leukocytic infiltration, high vascular density, thickening of the colon wall; 4, transmural infiltration, loss of goblet cells, high vascular density, thickening of the colon wall.

### Real-time RT-PCR assay

Messages of PIR-A and PIR-B from SI-derived DC subsets were determined by real-time RT-PCR. Total RNA of each sample was isolated by using the Isogen reagent (Nippon Gene, Japan) according to the manufacturer's instructions. The eluted RNA was quantified using an ND-1000 spectrophotometer (NanoDrop Technologies, Inc., Wilmington, DE, USA). RNA amplification was performed using the MessageBOOSTER whole transcriptome cDNA synthesis kit (Epicentre, Madison, WI, USA) according to the manufacturer's instructions. Reverse transcription was performed with the MessageBOOSTER whole transcriptome cDNA synthesis kit (Epicentre, Madison, WI, USA) according to the manufacturer's instructions. Real-time PCR was performed in a Rotor-Genes Q cycler machine (Qiagen) using the Rotor-Genes SYBR Green PCR kit (Qiagen), according to the manufacturer's instructions, in a total volume 20 μl. Cycling conditions for two target and GAPDH genes were 10 min at 95°C, 40 cycle of 5 s at 95°C, 15 s at 56°C, 20 s at 72°C. To correlate the threshold (Ct) values from the amplification plots to copy number, a standard curve was generated and a nontemplate control was run with every assay.

The primer sequences were as follows:

*PIRa1* 5′-gtctcccaaaaggcccatcc-3′ 5′-tcgaaaggacgatgaggacca-3′

*PIRb* 5′-gcttcagtggaggacatgcaaa-3′ 5′-cctgagcctggagggttca-3′

*GAPDH* 5′-ggcattgctctcaatgacaa-3′ 5′-atgtaggccatgaggtccac-3′

### Statistical analysis

Differences between groups were examined for statistical significance using the Mann–Whitney test. Cumulative survival rate was calculated by the Kaplan–Meier method.

## Results

### Analyses of the expression of DC stage-specific surface molecules

As shown in Fig. 1a and in our previous paper [1], three subsets of DCs (PIR-A/B$^{high}$, PIR-A/B$^{med}$, and PIR-A/B$^{-}$) were clearly observed in the CD11c$^{+}$/B220$^{-}$ conventional DCs (cDCs) on day 3 (3 days after the induction of ileitis by TNBS), and the PIR-A/B$^{med}$ cDC subset significantly increased at the final stage of inflammation (on day 7). The profile of DC subsets on the expression of PIR-A/B was only observed in the DCs of lamina propria origin, but not in mesenteric lymph node (MLN) DCs (Fig. 1b). Since the 6C1 antibody, which was used to detect the expression of PIR-A/B in this study, reacts with common epitopes of PIR-A and PIR-B, we did not distinguish the expression of PIR-A from that of PIR-B on the DC subsets. However, we evaluated the expression of PIR-B by using mAb against PIR-B. PIR-B was highly expressed on PIR-A/B$^{med}$ cDCs and equivalently on PIR-A/B$^{high}$ cDCs (Fig. 1c). SI-derived cDCs were clearly separated into two cDC populations (PIR-B$^{high}$ and PIR-B$^{low}$).

To distinguish the expression of PIR-A from that of PIR-B on cDCs, a quantitative real-time RT-PCR assay was carried out. Since the mAb specific for PIR-A is not yet available, we used mAb (clone 326414) that specifically recognizes PIR-B. We first purified PIR-B$^{high}$ cDCs and PIR-B$^{med}$ cDCs by a FACSAria after staining the cDCs with FITC-anti-CD11c mAb, PE-anti-PIR-B mAb (clone 326414), and APC-anti-B220 mAb, and the expression of PIR-A (and also PIR-B) in the PIR-B$^{high}$ cDCs and PIR-B$^{med}$ cDCs thus prepared was examined by a quantitative real-time RT-PCR assay. As shown in Fig. 1d, the message of PIR-A was clearly detected in the PIR-B$^{high}$ cDCs and also in the PIR-B$^{med}$ cDCs on day 7; the message level of PIR-A in the PIR-B$^{high}$ cDCs was higher than that in the PIR-B$^{med}$ cDCs. These findings strongly indicate that PIR-A/B$^{high}$ cDCs and PIR-A/B$^{med}$ cDCs used in our experiments co-expressed both PIR-A and PIR-B.

We then examined the expression of CD103, $CX_3CR1$, and CD11b on these SI-derived cDCs to further characterize the cDC subsets. As shown in Fig. 1e, PIR-A/B$^{med}$ cDCs were divided into CD103$^{high}$ and CD103$^{low}$ subsets, characterized by low expression of CD11b and $CX_3CR1$, whereas PIR-A/B$^{high}$ cDCs were mainly CD103$^{-}$$CX_3CR1^{low/-}$CD11b$^{high}$, and PIR-A/B$^{-}$ cDCs were $CX_3CR1^{-}$CD11b$^{low/-}$. Though PIR-A/B$^{-}$ cDCs are mainly CD103$^{high}$, a number of CD103$^{-}$ cells exist in this fraction.

The stimulatory activities of CD103$^{low}$PIR-A/B$^{med}$ cDCs and CD103$^{high}$PIR-A/B$^{med}$ cDCs were examined in MLR, and as shown in Fig. 2, the stimulatory activity of CD103$^{low}$PIR-A/B$^{med}$ cDCs was as low as that of CD103$^{high}$PIR-A/B$^{med}$ cDCs or of PIR-A/B$^{med}$ cDCs, suggesting that both subsets in PIR-A/B$^{med}$ cDCs have equal regulatory activity.

Furthermore, the expression level of CCR7 remained unchanged and low on the PIR-A/B$^{med}$ cDCs throughout the inflammatory processes (Fig. 1f). Therefore, we suspect

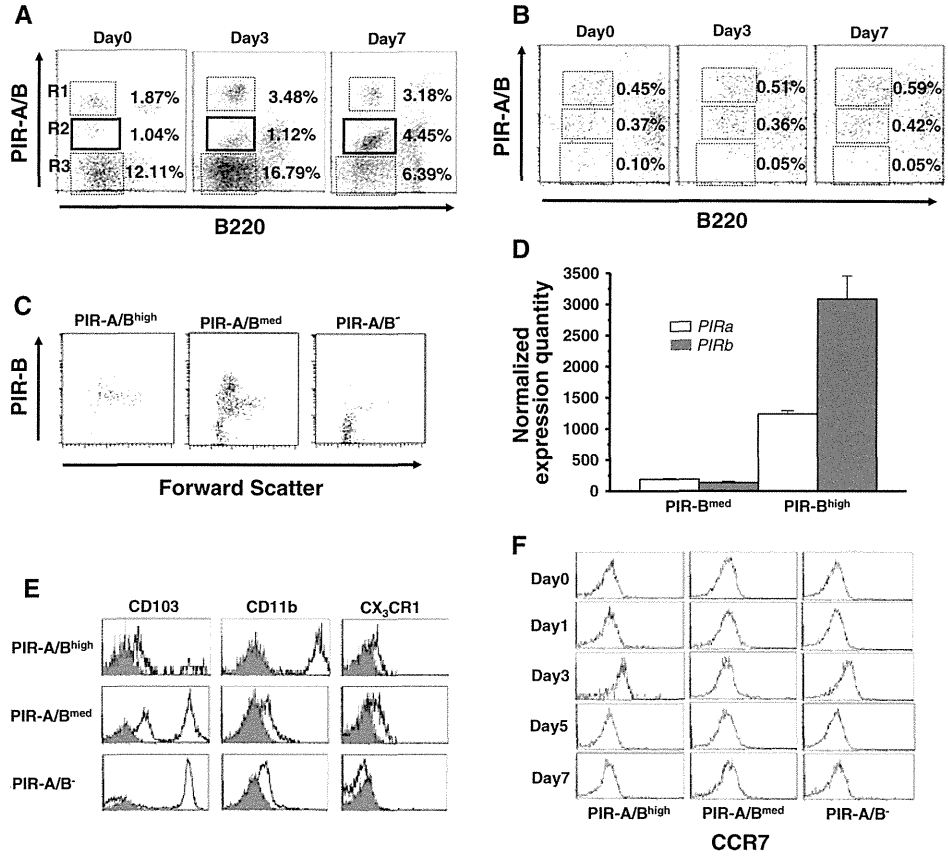


**Fig. 1** **a** Expression of PIR-A/B on SI-derived DCs. A DC-enriched population was prepared from the small intestine and stained with FITC-anti-CD11c, PE-anti-PIR-A/B, and APC-anti-CD45R mAbs. SI-derived cDCs (gated as $CD11c^{+}/B220^{-}$ cells) were separated into 3 populations on the basis of the expression of PIR-A/B: PIR-$A/B^{high}$ (gated as R1), PIR-$A/B^{med}$ (gated as R2), and PIR-$A/B^{-}$ (gated as R3). The results are representative of 5 replicate experiments. Frequencies of these cDC subsets were analyzed in viable cells from lamina propria of the small intestine. **b** Expression of PIR-A/B on MLN-derived DCs. A DC-enriched population was prepared from the MLNs and stained with FITC-anti-CD11c, PE-anti-PIR-A/B, and APC-anti-CD45R mAbs. MLN-derived cDCs were defined as $CD11c^{+}/B220^{-}$ cells. MLN-derived cDCs were separated into 3 populations on the basis of the expression of PIR-A/B. The results are representative of 5 replicate experiments. Levels of these cDC subsets were analyzed in viable cells from MLN. **c** Expression of PIR-B on DCs. The expression of PIR-B on cDC subsets prepared from the small intestine was analyzed by flow cytometry. The results are representative of 3 replicate experiments. **d** Expression of PIR-A and PIR-B in cDCs by a quantitative RT-PCR. The PIR-$B^{high}$ cDCs and PIR-$B^{med}$ cDCs were purified by a FACSAria after the staining of cDCs with FITC-anti-CD11c mAb, PE-anti-PIR-B mAb, and APC-anti-B220 mAb, and the expression of PIR-A and PIR-B in the PIR-$B^{high}$ cDCs and PIR-$B^{med}$ cDCs was examined by a quantitative real-time RT-PCR assay. *Open columns* represent the expression levels of PIR-A mRNA and *closed columns* represent those of PIR-B mRNA. Each *column* shows mean ± SD of 3 experiments. **e** Analyses of the expression of DC stage-specific surface molecules. A DC-enriched population prepared from the small intestine on day 7 after the injection of TNBS was analyzed by flow cytometry. The expression of CD103, $CX_3CR1$, and CD11b on the PIR-$A/B^{med}$ cDCs ($CD11c^{+}/B220^{-}$ cells) was compared with that on the PIR-$A/B^{high}$ or PIR-$A/B^{-}$ cDCs. *Filled gray histograms* represent isotype control. The results are representative of 3 replicate experiments. **f** Expression of CCR7 on DCs. The expression of CCR7 on cDC subsets prepared from the small intestine on days 0, 1, 3, 5, and 7 after the injection of TNBS was analyzed by flow cytometry. The results are representative of 3 replicate experiments

that PIR-$A/B^{med}$ cDCs do not migrate to the MLNs and could be a resident DC subset in the lamina propria.

## Prevention of TNBS-induced colitis by PIR-$A/B^{med}$ cDCs

To examine whether SI-derived PIR-$A/B^{med}$ cDCs actually ameliorate (or prevent) the TNBS-induced colitis, the adoptive cell transfer of PIR-$A/B^{med}$ cDCs into the recipient mice was performed at the time when TNBS was injected. SI-derived PIR-$A/B^{high}$ cDCs and PIR-$A/B^{-}$ cDCs, obtained from the ileitis-induced mice 1 day after the injection of TNBS, were used as controls. The overall survival rate of recipients of intraperitoneally injected PIR-$A/B^{med}$ cDCs was higher than that of the recipients of PIR-$A/B^{high}$ cDCs or PIR-$A/B^{-}$ cDCs (Fig. 3a). The body weight of the recipients of the PIR-$A/B^{med}$ cDCs remained unchanged after the injection of TNBS, whereas decreases in body weight were

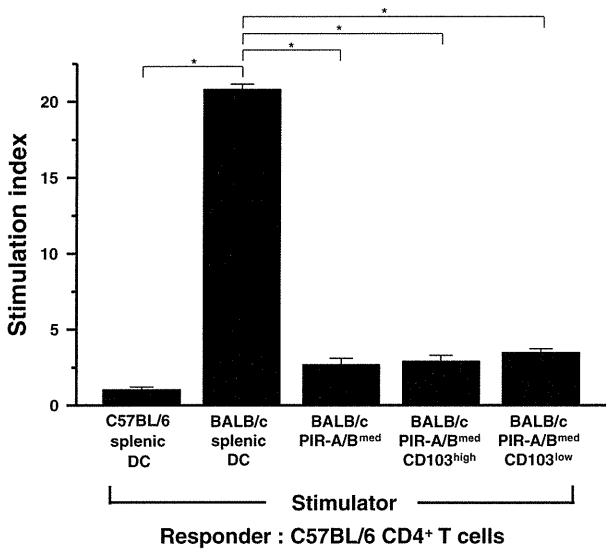


**Fig. 2** Stimulatory activity of $CD103^{low}$PIR-$A/B^{med}$ cDCs and $CD103^{high}$PIR-$A/B^{med}$ cDCs. A DC-enriched population was prepared from the small intestine on day 7 after the injection of TNBS, and $CD103^{low}$PIR-$A/B^{med}$ cDCs, $CD103^{high}$PIR-$A/B^{med}$ cDCs, and PIR-$A/B^{med}$ cDCs cDCs were sorted after the staining with FITC-anti-CD11c, PE-anti-CD103, and PE/Cy7-anti–B220, and APC-anti-PIR-A/B mAbs. Splenic cDCs prepared as $CD11c^+/CD3^-/B220^-$DCs were used as positive control DCs. The responder splenic $CD4^+$ T cells ($2 \times 10^4$) from C57BL/6 mice were cultured with $10^3$ various stimulator DCs for 72 h and pulsed with 0.5 μCi of [$^3$H]thymidine for the last 16 h of the culturing period. *Bars* represent the mean ± SDs of 3 mice, and the results are representative of 2 replicate experiments. $*P < 0.05$

observed in both the recipients of PIR-$A/B^{high}$ cDCs and PIR-$A/B^-$ cDCs (Fig. 3b). This was the case when the ratio of colon weight to body weight was determined on day 7 (Fig. 3c). Shortening of the colon length and thickening of the colon wall were clearly observed in the mice that received PIR-$A/B^{high}$ cDCs and PIR-$A/B^-$ cDCs (Fig. 3d). However, these macroscopical changes were not remarkable in the recipients of PIR-$A/B^{med}$ cDCs. As shown in Fig. 3e, the macroscopical scores for the colons of the mice that received PIR-$A/B^{med}$ cDCs were significantly lower than those that received PIR-$A/B^{high}$ cDCs and PIR-$A/B^-$ cDCs. The histological appearance of the colon was also assessed on days 3 and 7. Though infiltration of inflammatory cells, ulcerations, loss of cryptal cells, and thickening of the colon wall were clearly observed in the recipients of PIR-$A/B^{high}$ cDCs, PIR-$A/B^-$ cDCs, and PIR-$A/B^{med}$ cDCs 3 days after the injection of TNBS, these inflammatory injuries were markedly improved only in the recipients of PIR-$A/B^{med}$ cDCs on day 7, but neither in those that received PIR-$A/B^{high}$ cDCs nor those that received PIR-$A/B^-$ cDCs (Fig. 4a). This was also the case when the histopathological scores were determined (Fig. 4b). The colon from the mouse injected with 50% ethanol alone served as a normal control, and showed no evidence of inflammation. These findings clearly demonstrate the preventative effect of SI-derived PIR-$A/B^{med}$ cDCs in the progression of TNBS-induced colitis.

## Treatment of TNBS-induced colitis by PIR-$A/B^{med}$ cDCs

The adoptive cell transfer of PIR-$A/B^{med}$ cDCs into the recipient mice with TNBS-induced colitis was performed 3 days after the injection of TNBS to examine the curative effect of this unique DC subset. As shown in Fig. 5a, a decrease in body weight was observed after the injection of TNBS in all the mice treated. When PIR-$A/B^{med}$ cDCs, but not PIR-$A/B^{high}$ cDCs or PIR-$A/B^-$ cDCs, were transferred to these mice, their body weight gradually increased and reached the normal level on day 7. This was confirmed when the ratio of colonic to body weight was determined on day 7 (Fig. 5b).

Shortening of the colon length and thickening of the colon wall were clearly observed in the mice that received PIR-$A/B^{high}$ cDCs and PIR-$A/B^-$ cDCs (Fig. 5c). However, these macroscopical changes, observed at the onset of colitis, were ameliorated by the intraperitoneal injection of PIR-$A/B^{med}$ cDCs (Fig. 5d). The macroscopic scores also supported the therapeutic role of PIR-$A/B^{med}$ cDCs (Fig. 5e). When the histopathological scores were determined, infiltration of inflammatory cells, ulceration, loss of cryptal cells, and thickening of the colon wall were observed on day 3. These inflammatory injuries were markedly improved by day 7, by the intraperitoneal injection of PIR-$A/B^{med}$ cDCs (Fig. 6a), and this was also supported by assessing the histopathological scores (Fig. 6b).

These findings demonstrate the therapeutic role of PIR-$A/B^{med}$ cDCs after the onset and progression of TNBS-induced colonic inflammation.

## Migration of PIR-$A/B^{med}$ cDCs into the inflamed colon

To determine whether the transferred SI-derived cDCs migrate into the inflamed colon, $PIR^{med}$ cDCs prepared from the ileitis-induced mice were labeled with CFSE. The labeled cells were then transferred into the recipients at the time when colitis was induced by TNBS. As shown in Fig. 7, CFSE-labeled cells were clearly in the lamina propria and the submucosa of the colon 3 days after the induction of colitis. This result suggests that the transferred $PIR^{med}$ cDCs migrate into the colon and suppress the inflammatory response through the regulation of T cell proliferation and/or activation.

## Effect of Inhibition of IDO on the treatment of TNBS-induced colitis by PIR-$A/B^{med}$ cDCs

We next assessed whether IDO is involved in the regulatory mechanism of SI-derived PIR-$A/B^{med}$ cDCs. Mice

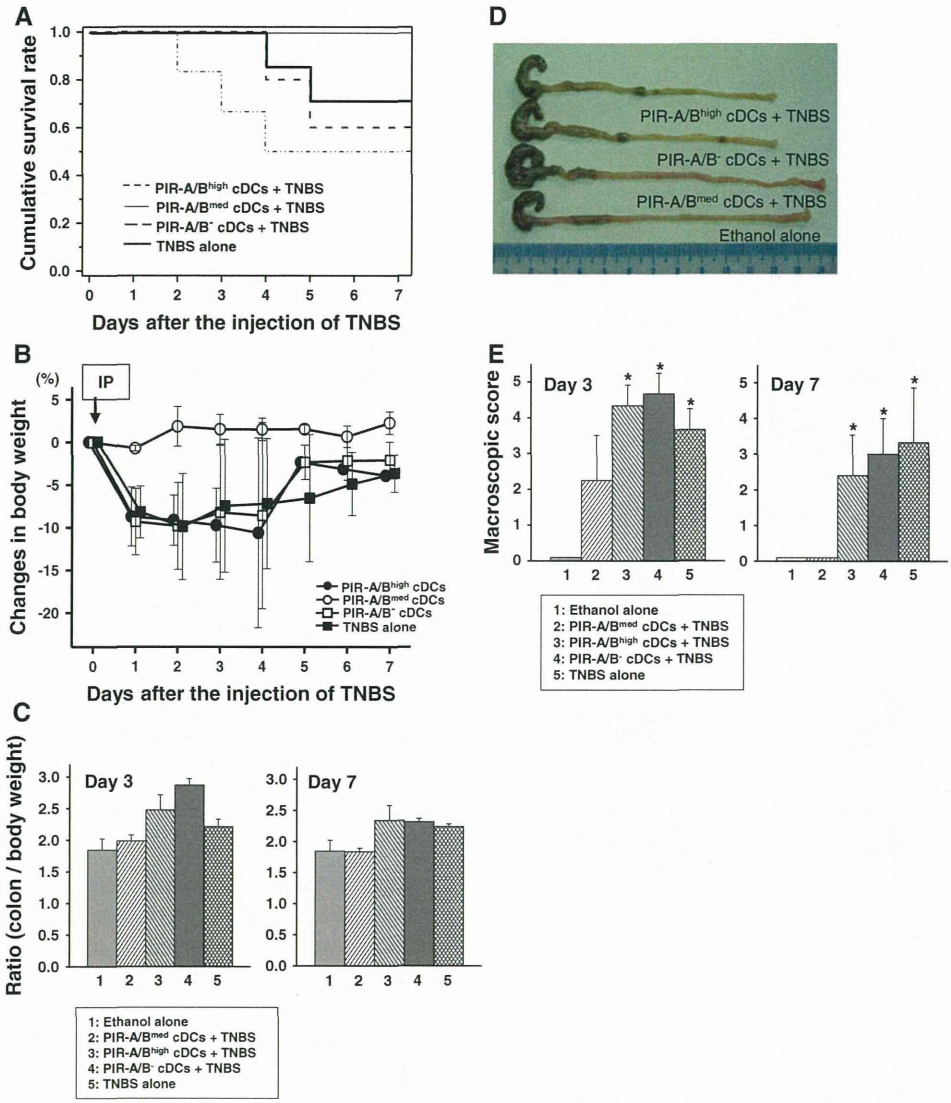


**Fig. 3** Prevention of TNBS-induced colitis by PIR-A/B$^{med}$ cDCs from the viewpoints of mortality, changes in body weight and colon weight, and macroscopical appearance. **a** Cumulative survival curves for recipients of the adoptive transfer of each cDC subset at the time when TNBS was injected. *Solid line* mice that received PIR-A/B$^{med}$ cDCs, *dashed line* mice that received PIR-A/B$^{high}$ cDCs, *dashed and dotted line* mice that received PIR-A/B$^{-}$ cDCs, *thick line* mice administered TNBS alone. The overall survival rate of recipients of PIR-A/B$^{med}$ cDCs was higher than that of those that received PIR-A/B$^{high}$ cDCs or PIR-A/B$^{-}$ cDCs. **b** Changes in body weight of mice that received each cDC subset at the time when TNBS was administered. Serial changes in body weight were measured daily throughout the experiment (day 0, before the injection of TNBS). Body weight of the recipients of PIR-A/B$^{med}$ cDCs remained unchanged after the injection of TNBS, whereas decreases in body weight were observed in both the recipients of PIR-A/B$^{high}$ cDCs and PIR-A/B$^{-}$ cDCs. *Symbols* and *bars* in the figure represent the mean ± SDs of 4 mice. (*Closed circles* mice that received PIR-A/B$^{high}$ cDCs, *open circles* mice that received PIR-A/B$^{med}$ cDCs, *open squares* mice that received PIR-A/B$^{-}$ cDCs, *closed squares* mice administered TNBS alone.) **c** The ratio of colonic to body weight was determined on days 3 and 7 after the injection of TNBS. Each *column* shows mean ± SD of 4 mice. **d**, **e** Macroscopical changes in the colons of mice that received each cDC subset. A representative photograph of colons from day 7 after the injection of TNBS (Fig. 3d). Shortening of the colon length and thickening of the colon wall were not remarkable in the recipients of PIR-A/B$^{med}$ cDCs. The colon from the mouse injected with 50% ethanol alone served as a normal control. Macroscopical scores of the colon from the mice that received PIR-A/B$^{med}$ cDCs were significantly lower than those from recipients that received PIR-A/B$^{high}$ cDCs and PIR-A/B$^{-}$ cDCs, particularly on day 7 (Fig. 3e). Each *column* shows mean ± SD of 4 mice. $*P < 0.05$ versus group 2

were intraperitoneally injected with 10 mg of IDO inhibitor, 1-mT, from day 3 after the injection of TNBS (at the time when SI-derived PIR-A/B$^{med}$ cDCs were transferred).

A shortening of the colon length and thickening of the colon wall were clearly observed even in the mice that received PIR-A/B$^{med}$ cDCs if 1-mT was simultaneously

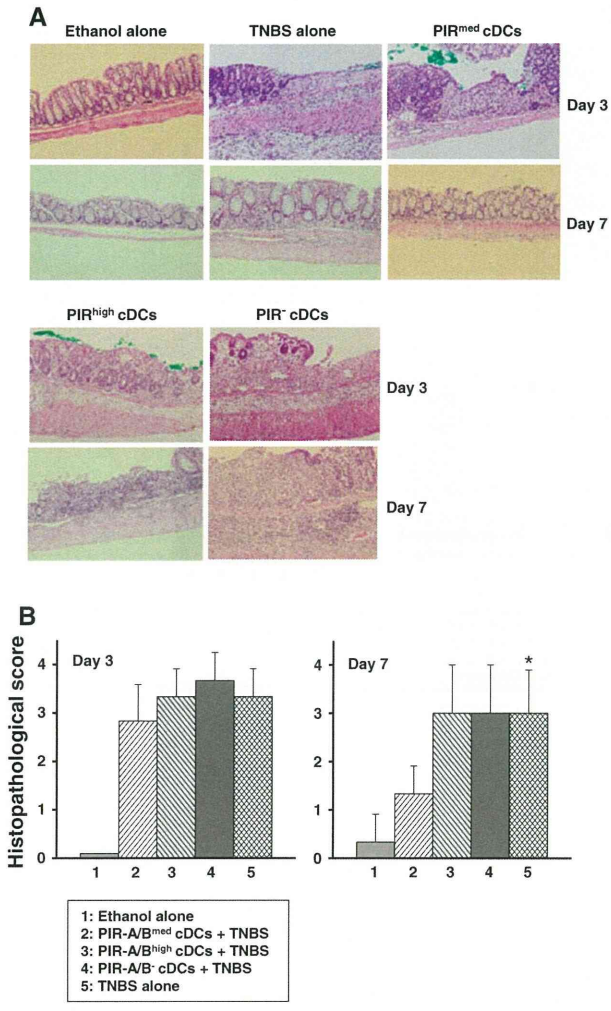


**Fig. 4** Prevention of TNBS-induced colitis by PIR-A/B$^{med}$ cDCs from the viewpoint of histological examination. **a** The tissue specimens were removed on days 3 and 7 after the injection of TNBS, and were fixed, embedded in paraffin, and the sections then stained with hematoxylin and eosin. Though infiltration of inflammatory cells, ulcerations, loss of cryptal cells, and thickening of the colon wall were clearly observed in the recipients of PIR-A/B$^{high}$ cDCs, PIR-A/B$^{-}$ cDCs, and PIR-A/B$^{med}$ cDCs 3 days after the injection of TNBS, these inflammatory injuries were markedly improved only in the recipients of PIR-A/B$^{med}$ cDCs on day 7, but neither in those that received PIR-A/B$^{high}$ cDCs nor those that received PIR-A/B$^{-}$ cDCs (×200). **b** Histopathological scores for the colons from the mice that received PIR-A/B$^{med}$ cDCs plus 1-mT. Each *column* shows mean ± SD of 4 mice. *$P < 0.05$ versus group 2

administered, being similar to those in the mice that received TNBS. Thus, significant gross morphologic differences were found between the colons of the mice that received PIR-A/B$^{med}$ cDCs plus 1-mT and those that received PIR-A/B$^{med}$ cDCs alone. Furthermore, the macroscopical scores—as indices of injury—for the colons from the mice that received PIR-A/B$^{med}$ cDCs plus 1-mT were significantly higher than those from the recipients of PIR-A/B$^{med}$ cDCs alone, as shown in Fig. 8b. This was

**Fig. 5** Treatment of TNBS-induced colitis by PIR-A/B$^{med}$ cDCs from the viewpoints of mortality, changes in body weight, the ratio of colonic to body weight, and macroscopical appearance. **a** Cumulative survival curves for recipients that received each cDC subset 3 days after the administration of TNBS. *Solid line* mice that received PIR-A/B$^{med}$ cDCs, *dashed line* mice that received PIR-A/B$^{high}$ cDCs, *dashed and dotted line* mice that received PIR-A/B$^{-}$ cDCs, *thick line* mice administered TNBS alone. The overall survival rate of recipients of PIR-A/B$^{med}$ cDCs was higher than that of those that received PIR-A/B$^{high}$ cDCs or PIR-A/B$^{-}$ cDCs. **b** Changes in body weight of mice that received each cDC subset 3 days after the administration of TNBS. Serial changes in body weight were measured daily throughout the experiment (day 0, before the injection of TNBS). *Symbols* and *bars* in the figure represent the mean ± SD of 4 mice. (*Closed circles* mice that received PIR-A/B$^{high}$ cDCs, *open circles* mice that received PIR-A/B$^{med}$ cDCs, *open squares* mice that received PIR-A/B$^{-}$ cDCs, *closed squares* mice administered TNBS alone). A decrease in body weight was observed after the injection of TNBS in all the mice treated. When PIR-A/B$^{med}$ cDCs were transferred to these mice, the body weight gradually increased and reached the normal level by day 7. **c** The ratio of colonic to body weight was determined on day 7 after the injection of TNBS. Each *column* shows mean ± SD of 4 mice. *$P < 0.05$ versus group 2. **d**, **e** Macroscopical changes in the colons from the mice that received each cDC subset. A representative photograph of colons from day 7 after the injection of TNBS is shown in Fig. 5d. Shortening of the colon length and thickening of the colon wall were not remarkable in the recipients of PIR-A/B$^{med}$ cDCs. The colon from the mouse injected with 50% ethanol alone served as a normal control. Macroscopical appearance observed at the onset of colitis was ameliorated by the intraperitoneal injection of PIR-A/B$^{med}$ cDCs (Fig. 5e). Each *column* shows mean ± SD of 4 mice. *$P < 0.05$ versus group 2

also the case when the histological appearance of the colon was assessed on day 7 (Fig. 8a, c). The infiltration of inflammatory cells, ulceration, loss of cryptal cells, and thickening of the colon wall were all observed in the recipients of PIR-A/B$^{med}$ cDCs plus 1-mT, but not in the mice that received PIR-A/B$^{med}$ cDCs alone (Fig. 8a, TNBS + PIR$^{med}$ cDCs vs. TNBS + PIR$^{med}$ cDCs + 1-mT). Furthermore, the mice treated with 1-mT alone, without the inoculation of the exogenous PIR-A/B$^{med}$ cDCs, showed exacerbated colitis (Fig. 8a, TNBS + 1-mT). It is noted that the regulatory effect of PIR-A/B$^{med}$ cDCs is significantly inhibited by "in vitro" treatment of DCs with 1-mT [Fig. 8a, TNBS + PIR$^{med}$ cDCs (treated with 1-mT)]. These results suggest that IDO, possibly derived from PIR-A/B$^{med}$ cDCs, might be involved in the suppression of inflammatory responses and in the inhibition of effector T cell function, resulting in the amelioration of TNBS-induced colitis by the adoptive transfer of SI-derived PIR-A/B$^{med}$ cDCs.

## Discussion

The pairing of activating and inhibitory receptors is thought to be necessary for the initiation, amplification, and termination of immune responses. Paired Ig-like receptors

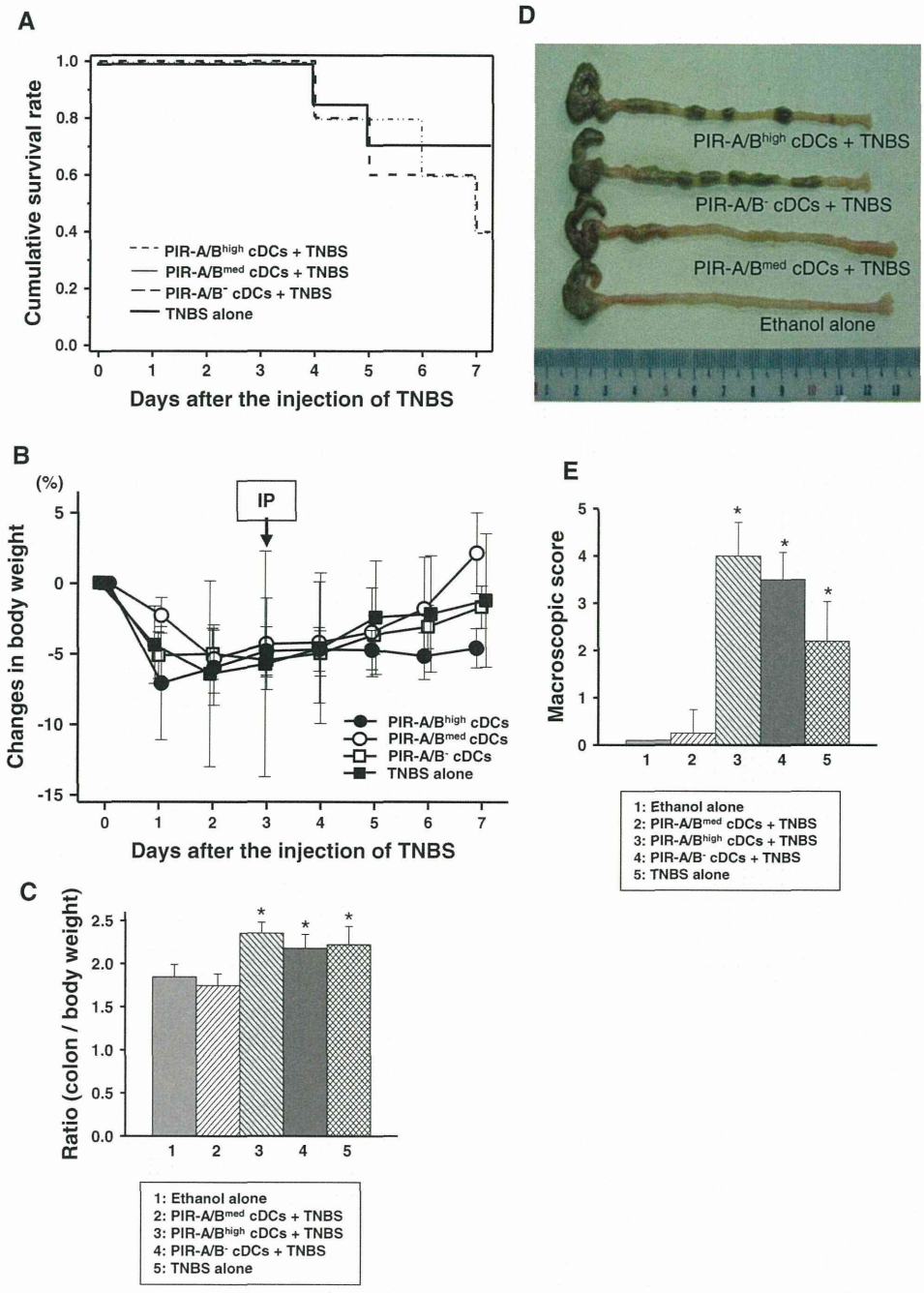


of activating (PIR-A) and inhibitory (PIR-B) isoforms in rodents are among the earliest paired receptors [12, 13]. It has been postulated that the disruption of PIR-A and PIR-B balance may affect their regulatory roles in host defense, including humoral immune, inflammatory, antigen-presenting, allergic, and coagulative responses, and there is increasing evidence that the balance of PIR-A and PIR-B functional activities is important for immune responses against bacterial infection. Actually the surface PIR-A level in the Salmonella-infected PIR-B$^{-/-}$ macrophage/Kupffer cells in the liver was enhanced [14]. In our previous paper, we focused on the expression of PIR on SI-derived DCs, and clarified the kinetic movement of DC subsets, based on the expression of PIR-A/B, in the lamina propria using the TNBS-induced ileitis model [1]. Three subsets of DCs (PIR-A/B$^{high}$, PIR-A/B$^{med}$, and PIR-A/B$^{-}$) in the CD11c$^{+}$/B220$^{-}$ cDCs were noted on day 3; only the number of PIR-A/B$^{med}$ cDCs increased when the inflammatory responses ceased on day 7. Additionally, in this paper, we assessed the expression levels of PIR-B using

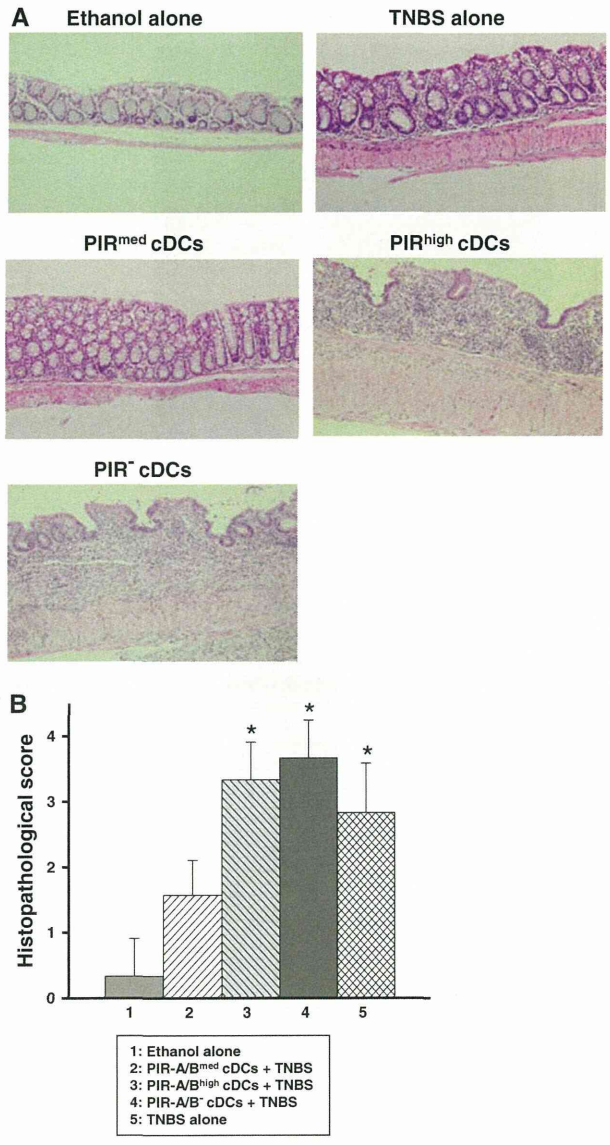


**Fig. 6** Treatment of TNBS-induced colitis by PIR-A/B$^{med}$ cDCs from the viewpoint of histological examination. **a** Representative histological findings in mice with TNBS-induced colitis as assessed by the inoculation of PIR-A/B$^{med}$ cDCs. Though infiltration of inflammatory cells, ulceration, loss of cryptal cells, and thickening of the colon wall were observed in the recipients of PIR-A/B$^{high}$ cDCs, and PIR-A/B$^{-}$ cDCs 7 days after the injection of TNBS, these inflammatory injuries were markedly improved by the intraperitoneal injection of PIR-A/B$^{med}$ cDCs (×200). **b** Histopathological scores for the colons from the mice that received PIR-A/B$^{med}$ cDCs plus 1-mT. Each *column* shows mean ± SD of 4 mice. *$P < 0.05$ versus group 2

specific mAb against PIR-B. PIR-B was highly expressed on PIR-A/B$^{med}$ cDCs and equivalently on PIR-A/B$^{high}$ cDCs. Although the expression frequency of PIR-A and PIR-B has not yet been determined in our study, PIR-A/B$^{med}$ cDCs have at least the PIR-B receptor, and PIR-B might influence the regulatory functions of PIR-A/B$^{med}$ cDCs, as has been reported in the *PIR-B*$^{-/-}$ mouse [15]. Furthermore, both PIR-B$^{high}$ cDCs and PIR-B$^{med}$ cDCs expressed PIR-A mRNA when determined by a quantitative RT-PCR, indicating that PIR-A/B$^{high}$ cDCs and PIR-A/B$^{med}$ cDCs co-expressed both PIR-A and PIR-B. Here, we have further characterized these DC subsets by the expression of other surface molecules related to the recruitment of DCs. PIR-A/B$^{med}$ cDCs were CD103$^{+}$CX$_3$CR1$^{-}$CD11b$^{-}$, and it is noted that CD103$^{+}$ DCs have been reported to migrate into the draining MLNs, where they promote the conversion of naïve T cells to Foxp3$^{+}$ regulatory T (Treg) cells in a retinoic acid (RA)- and TGF-$\beta$-dependent manner [5–7]. In our study, PIR-A/B$^{-}$ cDCs, in spite of their expression of CD103 (CD103$^{+}$CX$_3$CR1$^{-}$CD11b$^{-}$ subset, Fig. 1e), did not show the regulatory activity nor ameliorate the colitis. Thus, it can be speculated that the CD103$^{+}$PIR-A/B$^{-}$ cDCs could not sufficiently induce the iTregs, and that part of, or a subset of, CD103$^{+}$ DCs have such a regulatory function, and here we can identify the DC subset to be in charge of the regulatory function as CD103$^{+}$PIR-A/B$^{med}$ cDCs. Furthermore, two populations were detected in the PIR-A/B$^{med}$ cDCs as to the expression of CD103 (CD103$^{high}$PIR-A/B$^{med}$ cDCs and CD103$^{low}$PIR-A/B$^{med}$ cDCs in Fig. 1c). The stimulatory activity of CD103$^{low}$PIR-A/B$^{med}$ cDCs was as low as that of CD103$^{high}$PIR-A/B$^{med}$ cDCs, when determined in allogeneic MLR. Thus, it is feasible that both subsets in PIR-A/B$^{med}$ cDCs have equal regulatory activity.

The profile of DC subsets on the expression of PIR-A/B was only observed in the DCs of lamina propria origin, not in MLN DCs, and the expression of CCR7, the important chemokine receptor for the migration of DCs, remained unchanged on the PIR-A/B$^{med}$ cDCs throughout the inflammatory processes (Fig. 1f). These findings strongly suggest that the PIR-A/B$^{med}$ cDCs are resident DCs in the lamina propria.

As to the functional aspect of this DC subset, the expression of costimulatory molecules such as CD86 and CD54 was lower in the PIR-A/B$^{med}$ DCs compared with the other two cDC subsets or splenic DCs. Furthermore, the stimulatory activity of PIR-A/B$^{med}$ cDCs was lower than that of PIR-A/B$^{high}$ or PIR-A/B$^{-}$ cDCs, and far lower than that of splenic DCs. In addition, an increase in the message level of IL-10 was clearly observed in the PIR-A/B$^{med}$ cDCs on day 7, whereas that of proinflammatory cytokines such as IL-6 and IL-12 was low. Therefore, we postulated that PIR-A/B$^{med}$ cDCs may be involved in the termination of the TNBS-induced ileitis by the delivery of anergic signals to effector T cells as a result of the lower expression of costimulatory molecules and the production of immunoregulatory cytokine [1]. In this paper, we have examined the regulatory effect of the PIR-A/B$^{med}$ cDC subset in vivo by the adoptive cell transfer of this DC subset into mice with TNBS-induced colitis. Mortality, changes in body

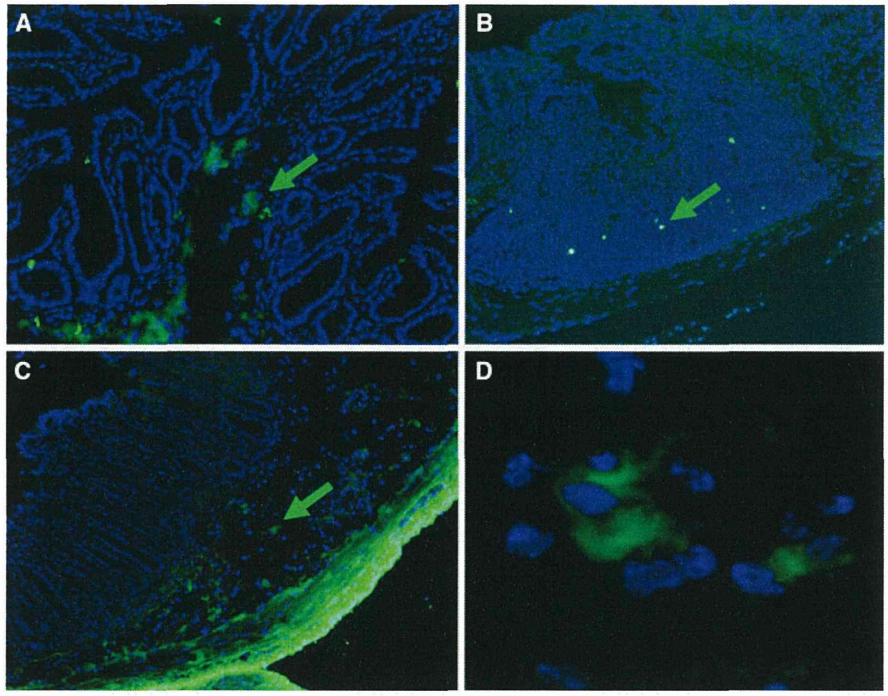


**Fig. 7** Migration of PIR-A/B$^{med}$ cDCs into the inflamed colon. PIR$^{med}$ cDCs prepared from the small intestine were labeled with CFSE and transferred into the recipients at the time when colitis was induced by TNBS. CFSE-labeled cells (*arrows, green*) were detected in the lamina propria and the submucosa of the colon on day 3 after the induction of colitis. Cellular nuclei were counterstained with DAPI (**a** ×200, **b** ×100, **c** ×100, **d** ×400)

weight, macroscopical appearance, and histological changes were markedly improved in the recipients of these PIR-A/B$^{med}$ cDCs, in contrast to these indicators in the control mice, suggesting the therapeutic role of PIR-A/B$^{med}$ cDCs. When examined using CFSE-labeled PIR-A/B$^{med}$ cDCs, these cells were clearly detected in the colon after their intraperitoneal transferr into the colitis-induced mice (Fig. 7), suggesting that they actually migrated into the inflamed colon and suppressed the inflammatory responses.

One of the feasible mechanisms by which the immune response is terminated is IDO-related. As is well accepted, IDO expression in DCs leads to the degradation of tryptophan and the concomitant build-up of several metabolites, referred to as kynurenines. Since activated T cells are dependent on tryptophan, the activation of IDO creates an environment that suppresses the immune system through the regulation of T cell proliferation and survival. In addition, the metabolites, such as kynurenine, themselves have a direct effect on T cells, including promoting their differentiation into Tregs [16, 17] and altering the balance of Th1 versus Th2 responses [16, 18]. Thus, IDO, whether through tryptophan depletion or through the production of its metabolites, can negatively regulate various aspects of T cell function in that it can lead to anergy, arrested cell cycle, altered cytokine production, and/or make T cells susceptible to apoptosis [16, 19–23]. Recent research indicates that the production of IDO by DCs actually inhibits T cell proliferation through tryptophan degradation [24, 25], and IDO has been reported to be expressed in the normal colon and upregulated in the setting of TNBS colitis. Furthermore, it has been reported that the inhibition of IDO during TNBS colitis resulted in increased mortality and an augmentation of the normal inflammatory response [26]. In humans, upregulation of IDO was observed in mucosa samples from patients with active inflammatory bowel disease [26–28].

In this study, we found that colitis was greatly exacerbated when the mice were treated with 1-mT at the time PIR-A/B$^{med}$ cDCs were transferred. That is, the therapeutic ability of PIR-A/B$^{med}$ cDCs is decreased by inhibition of IDO. Thus, a decrease in tryptophan or its degradative metabolites, both of which are dependent on IDO in PIR-A/B$^{med}$ cDCs, might be directly involved in the negative regulation of effector T cells, resulting in the amelioration of TNBS-induced colitis. Furthermore, the mice treated with 1-mT alone, without the inoculation of the exogenous PIR-A/B$^{med}$ cDCs, showed exacerbated colitis, suggesting that this IDO inhibitor affects the function of gut "in situ" DCs that have the regulatory function. This was confirmed by the experiment in which PIR-A/B$^{med}$ cDCs were treated "in vitro" with 1-mT. Moreover, the therapeutic ability of PIR-A/B$^{med}$ cDCs is decreased by this treatment, indicating that the IDO inhibitor directly affects the immunoregulatory function of PIR-A/B$^{med}$ cDCs. In addition to this process, IDO-related metabolites may promote the differentiation into Tregs and alter the balance of Th1/Th2/Th17 cells, this also being a possible mechanism of IDO-related reduction of immune and inflammatory responses.

As has been well accepted, CX3CR1$^{+}$ DCs (and/or DCs bearing other chemokine receptors) extend processes